

## Cascaded second-order nonlinearity in an optical cavity

A. G. WHITE(\*), J. MLYNEK and S. SCHILLER(\*\*)

*Fakultät für Physik, Universität Konstanz - D-78434 Konstanz, Germany*

(received 22 April 1996; accepted in final form 3 July 1996)

PACS. 42.50-p – Quantum optics.

PACS. 42.65Ky – Harmonic generation, frequency conversion, parametric oscillation, and parametric amplification.

PACS. 42.65Pc – Optical bistability, multistability, and switching.

**Abstract.** – Phase-mismatched optical second-harmonic generation in a low-loss external enhancement cavity is used to generate an effective third-order nonlinearity for continuous-wave laser radiation. The threshold for optical bistability is calculated. The cascading effect is demonstrated by detecting bistability of the line shape of a low-loss monolithic MgO:LiNbO<sub>3</sub> resonator pumped by a Nd:YAG laser. The simplicity of cascaded  $\chi^{(2)}$  resonators makes the method particularly promising for quantum optics.

Third-order optical nonlinearities are of importance for both applied and fundamental research: in signal processing and communications it is for their potential to realize all-optical switching [1], whereas in the field of quantum optics they may be employed to manipulate the quantum fluctuations of light, in particular to generate nonclassical states of light [2] and perform quantum nondemolition measurements [3]. Central to these applications is the search for materials exhibiting large nonlinearities; in addition they must be environmentally stable and resistant to optical power. For quantum-optical use the media must also have a large ratio of nonlinearity to loss in order to suppress the influence of vacuum fluctuations. A variety of  $\chi^{(3)}$  media has been investigated, including vitreous silica, semiconductors, organic compounds, atomic beams, and cold atoms [2], [3]. Because of the limitations (complexity, stability) of these systems, the possibility [4] of using well-known second-order nonlinear materials for the same purposes has sparked a new direction of research [5]. A number of studies [6] have discussed or demonstrated various aspects of cascading effects in second-harmonic generation. All experiments reported up to date were performed in single-pass geometry, using pulsed lasers with high peak intensities to obtain sufficiently large responses.

The purpose of this letter is to show that cascaded second-order nonlinearities can be used to control low-power, continuous-wave light via optical bistability [7], occurring in phase-mismatched second-harmonic generation in a low-loss optical cavity [8]<sup>(1)</sup>.

We derive the response of a cascaded  $\chi^{(2)}$  nonlinear optical cavity (fig. 1) by first considering the propagation equations for the electric-field envelopes  $A_1$ ,  $A_2$  of the Gaussian waves of

---

(\*) Present address: Department of Physics, Australian National University, Canberra, ACT, 0200, Australia.

(\*\*) E-mail: stephen.schiller@uni-konstanz.de

<sup>(1)</sup> Bistability can occur in detuned  $\chi^{(2)}$  resonators also for perfect phase match: in doubly resonant SHG, an effective Kerr nonlinearity is predicted to occur if the harmonic wave is significantly detuned from resonance (see [9]); in pump-resonant parametric oscillation bistability has been observed by [10].

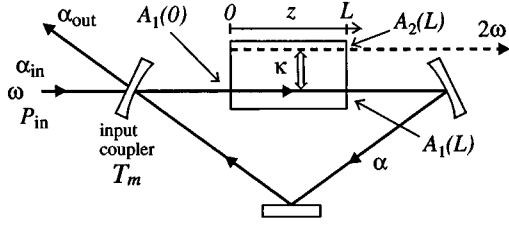


Fig. 1.

Fig. 1. – Schematic of cavity considered for resonantly enhanced cascaded second-harmonic generation.

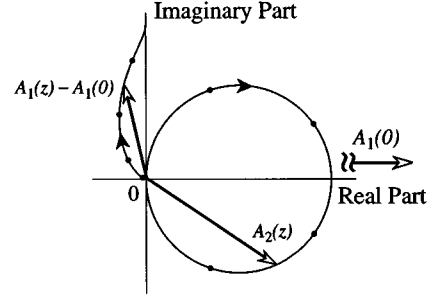


Fig. 2.

Fig. 2. – Phasor diagram of the evolution of the fundamental and harmonic electric-field amplitudes  $A_1, A_2$  along the medium under phase mismatch  $\Delta k L = 2\pi$ . The harmonic field at the end of the medium,  $A_2(L)$ , is zero, while the fundamental one has experienced a cascaded phase shift ( $A_1(L) - A_1(0)$  is imaginary) and nearly zero loss.  $A_1(0)$  is taken as real. The points are at intervals of  $L/5$  along  $z$ .

frequency  $\omega$  and  $2\omega$  in the nonlinear medium [11],

$$\frac{dA_1(z)}{dz} = i\frac{\kappa}{2}u^*(\Delta k, z)A_1^*(z)A_2(z), \quad \frac{dA_2(z)}{dz} = i\frac{\kappa}{2}u(\Delta k, z)A_1(z)^2. \quad (1)$$

The inclusion of a finite wave vector mismatch  $\Delta k = k(2\omega) - 2k(\omega)$  in the function  $u(\Delta k, z) = \exp[i\Delta k z]/(1 + i(z - L/2)/z_r)$  is central to the following discussion.  $u$  also describes the effects of focusing [12]. The Rayleigh ranges of the fundamental and harmonic waves are taken as equal,  $z_r = n\omega w^2/2c$ , since the difference between their indices of refraction remains small even for large  $\Delta k$ ,  $n_\omega \simeq n_{2\omega} \simeq n$ .  $w$  is the fundamental wave waist at the focus, located at  $z = L/2$ .  $\kappa \sim \chi^{(2)}$  is the nonlinear coefficient. The field envelopes and their powers are related by  $P = |A|^2 \pi z_r/2\mu_0 n$ ,  $\mu_0$  being the vacuum permeability.

Since the continuous-wave fields of interest here are weak, it is sufficient to integrate eq. (1), with the initial condition  $A_2(0) = 0$  over the length  $L$  of the medium to second order in  $\kappa$ ,

$$A_1(L) - A_1(0) = -(\kappa L/2)^2 K |A_1(0)|^2 A_1(0)/2, \quad A_2(L) = i(\kappa L/2) I A_1(0)^2. \quad (2)$$

The dimensionless coupling coefficients are  $K(\Delta k L) = 2 \int_0^L \int_0^z u^*(\Delta k, z) u(\Delta k, z') dz' dz / L^2$  and  $I(\Delta k L) = \int_0^L u(\Delta k, z) dz / L$ , related by  $\text{Re}K = |I|^2$ . The evolutions described by expressions (2) are pictorially represented in fig. 2. The subharmonic field envelope at the end of the medium,  $A_1(L)$ , has experienced both a nonlinear loss, *i.e.* second-harmonic generation ( $\sim \text{Re}K$ ), and a nonlinear phase shift,  $\sim \text{Im}K$ . The latter is an effective Kerr nonlinearity resulting from the cascaded  $\chi^{(2)}$  nonlinearity. The harmonic-wave amplitude is always nonzero on average inside the medium, but for the values  $\Delta k = \pm 2\pi m$  (assuming weak focusing,  $z_r \gg L$ ) it decreases to zero at its end, resulting in zero net harmonic power leaving the medium.

Figure 3 shows the dependence of  $K$  for weak focusing. The dispersive and absorptive parts of  $K$  resemble those of an atomic transition response. However, a  $\chi^{(2)}$  material is distinguished by the notable difference that the absorptive part exhibits discrete zeros at which the dispersive part is finite and large.

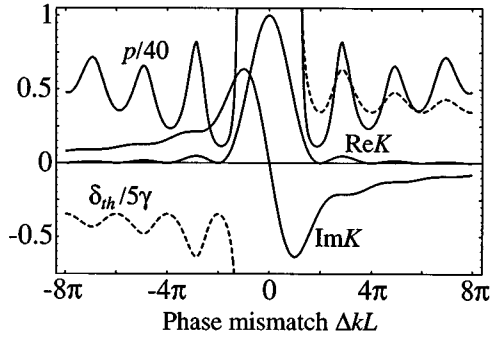


Fig. 3.

Fig. 3. – Calculated phase mismatch dependence of the conversion coefficient  $\text{Re}K$ , the nonlinear phase shift coefficient  $\text{Im}K$ , the normalized bistability threshold  $p$ , and the cavity detuning at threshold  $\delta_{\text{th}}$ . Plane-wave mode geometry is assumed.

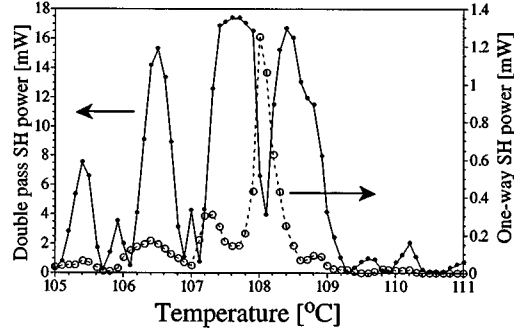


Fig. 4.

Fig. 4. – Phase matching curve for second-harmonic (SH) generation. Double-pass: total SH power leaving the crystal through the AR side; one-way: fraction of SH power generated on the first half of the round trip and transmitted through the nominally high-reflectivity mirror. Mode matched input 1064 nm power was 33 mW. Lines are guides for the eye.

Two central aspects arise in implementing an intra-cavity cascaded  $\chi^{(2)}$  nonlinearity. First, the nonlinear phase shift is enhanced by resonating the subharmonic wave  $\omega$ . Second, the nonlinear phase shift has a significant influence when it is on the order of the round-trip propagation phase shift corresponding to a detuning by one cavity linewidth, which is small for a low-loss cavity. As both the enhancement and the relative magnitude scale inversely with cavity losses, these play a crucial role. For a quantitative description we consider a cavity as in fig. 1 for which the dynamics of the intracavity envelope  $\alpha = \sqrt{\tau}A_1(0)$  ( $\tau$  is the cavity round-trip time) is easily obtained by imposing a self-consistency condition for it at the input coupler mirror [9]. The result is

$$\dot{\alpha} = -\left[\gamma + i\delta + \frac{\mu}{2}K|\alpha|^2\right]\alpha + \sqrt{2\gamma_c}\alpha_{\text{in}}. \quad (3)$$

Here,  $\mu = (\kappa L/2\tau)^2$  is the interaction strength,  $\alpha_{\text{in}} = A_{1,\text{in}}$  is the external input field, and  $\delta$  is the detuning between  $\omega$  and the cavity resonance frequency. The coupling and total decay rates for the intracavity field are defined as  $\gamma_c = T_m/2\tau$ ,  $\gamma = \gamma_c + S/2\tau$ , respectively, where  $T_m$  is the input mirror transmission and  $S$  are any linear round-trip losses. In the above equation, the pure-SHG part of the  $\chi^{(2)}$ -interaction,  $\text{Re}K$ , represents an intensity-dependent loss, which leads to power broadening of the cavity linewidth. The Kerr phase shift term  $\propto \text{Im}K$  results in an intensity-dependent detuning of the cavity mode and a distortion of the lineshape of the cavity resonance. Optical bistability is reached when the linear ( $\delta$ ) and nonlinear detunings are of opposite sign and the latter is large enough. The threshold input power required ( $P_{\text{in}}^{\text{th}}$ ) is found by solving eq. (3) in the steady-state case under the condition of infinite slope in the cavity lineshape,  $(d|\alpha|^2/d\delta)^{-1} = 0$ ,

$$P_{\text{in}}^{\text{th}} = \frac{T_m + S}{T_m} \frac{(T_m + S)^2}{4\Gamma_{\text{SHG}}} \text{Max}(\text{Re}K)p(\Delta kL), \quad p(\Delta kL) = \frac{8}{3\sqrt{3}} \frac{|K|^2}{(|\text{Im}K| - \sqrt{3}\text{Re}K)^3}. \quad (4)$$

In eq. (4) we have recast the bistability power scale in terms of measurable parameters,  $\Gamma_{\text{SHG}}$

being the power conversion coefficient for SHG at the peak of the phase matching curve, where  $\text{Re}K$  takes on its maximum,  $\Gamma_{\text{SHG}} = 2\mu_0 n \mu \tau^2 \text{Max}(\text{Re}K)/\pi z_r$ . Recalling for comparison that the  $2\omega$  threshold power required to achieve parametric oscillation is  $(T_m + S)^2/4\Gamma_{\text{SHG}}$ , we note that the bistability power at  $\omega$  is  $\simeq p$  times larger. Thus, the bistability power scales as the square of the ratio of second-order nonlinearity  $\chi^{(2)}$  and total cavity loss  $T_m + S$ .

An important result contained in eq. (4) is that cascaded bistability can only occur for wave vector mismatches such that  $|\text{Im}K| > \sqrt{3}\text{Re}K$ . Figure 3 shows the dependence of the normalized threshold on  $\Delta kL$ , assuming a weakly focused resonator mode. The threshold is minimum near  $\Delta kL = \pm 2\pi$ , where the SHG efficiency  $\text{Re}K$  vanishes. For large wave vector mismatch the threshold power increases approximately linearly with  $|\Delta kL|$ . Also indicated in fig. 3 is the detuning  $\delta_{\text{th}} = \delta(P_{\text{in}} = P_{\text{in}}^{\text{th}}) = -\text{sgn}(\text{Im}K) (\sqrt{3}|\text{Im}K| + \text{Re}K)/(|\text{Im}K| - \sqrt{3}\text{Re}K)$  at which the vertical slope of the cavity lineshape occurs. Note that  $\delta_{\text{th}}$  has the same sign as the wave vector mismatch.

For the experimental demonstration of the cascaded  $\chi^{(2)}$  nonlinearity with continuous-wave light, special attention must be paid to achieving small cavity losses and large nonlinearity. We have selected the well-tested crystal  $\text{MgO:LiNbO}_3$  as the nonlinear medium since it exhibits a large  $\chi^{(2)}$  for SHG of 1064 nm ( $\omega$ ) radiation as well as low bulk absorption and scatter loss. The wave vector mismatch  $\Delta kL$  is controllable by varying the temperature ( $T$ ) of the crystal relative to the phase matching peak at about 108°C, with a tuning coefficient  $\partial\Delta k/\partial T = 7.5$  rad/(cm K). The optical cavity is a miniature monolithic standing-wave cavity whose mirrors are dielectric coatings deposited directly on the 10 mm radius convexly polished end faces of the 7.5 mm long crystal. The cavity mode is thus confined entirely within the crystal. From the measured finesse and the on-resonance reflectivity a round-trip loss  $S = 0.3\%$  and a mirror transmission  $T_m = 0.33\%$  at 1064 nm are deduced. The input mirror is antireflection coated for 532 nm. The back mirror is highly reflective at both 532 nm and 1064 nm. The pump wave  $\omega$  is provided by a tunable, single-frequency Nd:YAG laser.

Figure 4 shows the temperature dependences of the 532 nm harmonic power generated on the first half and over the full distance of the round trip inside the cavity. We remark that the efficiency curves differ from the theoretical behaviour ([13], cf. also  $\text{Re}K$  in fig. 3) for several reasons: for the input power level used, the harmonic output power is not strictly proportional to  $\text{Re}K$ ; temperature inhomogeneities within the crystal are present; and, a differential phase shift between the fundamental and harmonic waves occurring at the high reflector leads to significant interference effects [14]. The presence of these is visible from the substantial difference between the one-way and round-trip traces. Following the above plane-wave analysis, the minimum bistability threshold is expected where the external conversion efficiency is near zero. The measured round-trip SHG efficiency in fig. 4 exhibits near-zero minima, which are, therefore, chosen as the operating points for the observation of the cascading effect. Note that the round-trip conversion efficiency at the phase matching peak is  $\simeq 50\%$ . A SHG coefficient  $\Gamma_{\text{SHG}} \simeq 2/\text{kW}$  is inferred from this result, leading to an estimated minimum bistability power on the order of 45 mW, assuming the plane-wave result to be applicable.

Figure 5 *i*), *ii*) show the behaviour of the line shape of the cavity mode at high input power (125 mW) as the laser is detuned back and forth. The data was obtained by recording the 1064 nm power transmitted through the nominally highly reflecting mirror, which is proportional to  $|\alpha|^2$ . A fast laser frequency scan (12 MHz/ $\mu\text{s}$ ) is used so as to attenuate the influence of thermal effects, where absorption of circulating power and resulting heating and expansion of the cavity causes leaning to negative detuning, irrespective of crystal temperature and  $\Delta k$ . As a baseline scan, fig. 5 *i*) shows the lineshape when the doubler is operated at room temperature where the phase mismatch is extremely large. With the crystal temperature adjusted for maximum SHG efficiency, a significant broadening due to the conversion loss  $\mu\text{Re}K|\alpha|^2/2$  and a corresponding

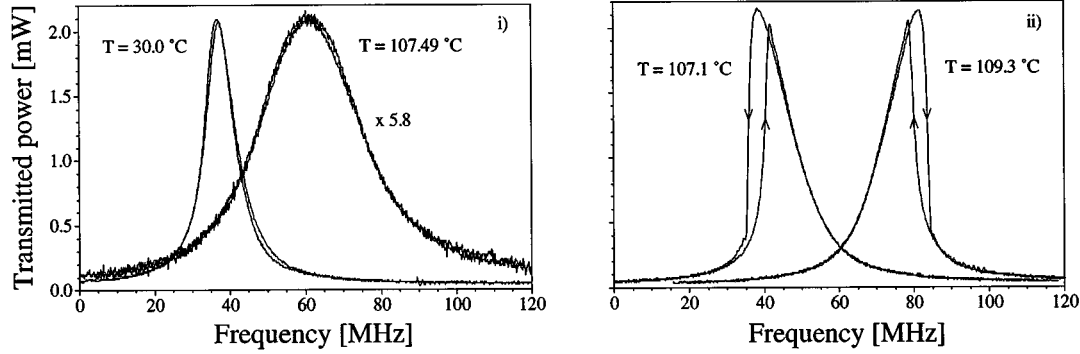


Fig. 5. – Lineshapes of the TEM<sub>00</sub> resonator mode. *i*) no cascaded nonlinearity:  $T = 30^\circ\text{C}$ , zero nonlinear loss;  $T = 107.49^\circ\text{C}$ , large nonlinear loss  $\text{Re}K$  causing line broadening; *ii*) no nonlinear loss:  $T = 107.1^\circ\text{C}$ , positive wave vector mismatch;  $T = 109.3^\circ\text{C}$ , negative wave vector mismatch. 1064 nm input power was 125 mW. The distinctly different forward and backward scans in *ii*) are evidence for optical bistability due to a cascaded  $\chi^{(2)}$  nonlinearity. Line positions are arbitrary.

reduction in circulating subharmonic power occurs; no significant asymmetry is observed, however. The observed broadening factor is consistent with the nonlinearity  $\Gamma_{\text{SHG}}$  and the cavity losses. With the temperature changed slightly from the phase matching peak so as to give nearly zero double-pass conversion efficiency (see fig. 2), the scans change dramatically as shown in fig. 5 *ii*). At the high input power level used the scans display hysteresis and are strongly asymmetric, leaning towards opposite detuning for opposite temperature change, *i.e.* wave vector mismatch, in agreement with the prediction for  $\delta_{\text{th}}$ . The data is consistent with the cavity being driven above bistability. The fact that line asymmetry is observed for both positive and negative wave vector mismatch at opposite detunings represents clear evidence that an effective Kerr nonlinearity due to cascaded second-order nonlinearity is at work. Small thermal effects are still present, as can be seen from the fact that the bistability is greater for negative wave vector mismatch. In the scans shown in fig. 5 *ii*), harmonic-power production was minimal (a few mW), which is also borne out by the fact that the peak subharmonic circulating power was nearly the same as for the cold cavity (fig. 5 *i*). The quantitative agreement between the input power required to reach bistability and the prediction of eq. (4) is satisfactory, considering that the double-pass phase matching curve of fig. 3 shows that the assumptions of a homogeneous nonlinear material and the absence of interference effects are not satisfied for the present resonator.

An undesired effect arising in this study is subharmonic-pumped parametric oscillation (SPO) [15]. This occurs when the average harmonic field  $2\omega$  in the nonlinear medium is sufficiently large to act as a pump wave for the generation of resonant nondegenerate signal and idler waves. The theoretically calculated subharmonic threshold power for SPO can be less than the bistability power  $P_{\text{in}}^{\text{th}}$ , even when  $\text{Re}K = 0$ : for this device SPO was observed at subharmonic input powers above 40 mW. For SPO to occur, the nondegenerate signal and idler waves must be resonant with sufficiently small detuning. It is possible to avoid SPO by carefully varying the operating temperature of the resonator and frequency of the laser, so that only the subharmonic is resonant and there are no suitable frequencies at which the idler and signal waves can resonate. However, this becomes increasingly difficult with higher subharmonic power.

In conclusion, we have presented a method for obtaining a  $\chi^{(3)}$  continuous-wave nonlinear optical system by means of temperature-detuned second-harmonic generation in a crystal. It is

simpler than continuous-wave methods based on atomic media. Furthermore, a large variety of nonlinear solid-state media is available that covers a very large spectral range; indeed, even media that are not phase-matchable for SHG may be used, since cascading is effective even for relatively large phase mismatch due to the linear, rather than quadratic, dependence of the bistability threshold on  $\Delta k$ . Since several cavity quantum-optical effects, such as squeezing [16], quantum nondemolition measurements [17], and noise-free amplification [18], have been predicted assuming self- or cross-Kerr interactions [19], an important extension of the present work is the demonstration that cascading can lead not only to a self-interaction, as studied here, but also, in phase-mismatched sum-frequency generation or type-II SHG, to an effective cross-Kerr coupling between two waves of different wavelength or polarization, respectively [20].

\*\*\*

We thank R. BRUCKMEIER, G. BREITENBACH and K. SCHNEIDER for stimulating discussions. Financial support has been provided by ESPRIT LTR Project 20029 ACQUIRE and the Deutscher Akademischer Auslandsdienst.

*Additional Remark.* – After the paper was refereed, we became aware of an experimental study (OU Z. Y., *Opt. Commun.*, **124** (1996) 430) of c.w. cascaded phase shifts. Bistability was not reached, however.

#### REFERENCES

- [1] STEGEMAN G. I. and MILLER A., in *Photonics in Switching*, edited by J. E. MIDWINTER, Vol. 1 (Academic Press) 1993, p. 81.
- [2] RAIZEN M. G. *et al.*, *Phys. Rev. Lett.*, **59** (1987) 198; HOPE D. M. *et al.*, *Phys. Rev. A*, **46** (1992) R1181; LAMBRECHT A. *et al.*, *Appl. Phys. B*, **60** (1995) 129.
- [3] MILBURN G. J. *et al.*, *J. Opt. Soc. Am. B*, **4** (1987) 1476; POIZAT J.-PH. and GRANGIER P., *Phys. Rev. Lett.*, **70** (1993) 71.
- [4] OSTROVSKII L. A., *J. Exp. Theor. Phys. Lett.*, **5** (1967) 272; THOMAS J.-M. R. and TARAN J.-P. E., *Opt. Commun.*, **4** (1972) 329.
- [5] DESALVO R. *et al.*, *Opt. Lett.*, **17** (1992) 28.
- [6] See references in: ASSANTO G. *et al.*, *J. Quantum Electron.*, **31** (1995) 673.
- [7] GIBBS H., *Controlling Light with Light* (Academic Press) 1985.
- [8] SCHILLER S. *et al.*, *Proc. SPIE*, edited by Y. SHEVY, Vol. **2378**, 1995, p. 91.
- [9] DRUMMOND P. *et al.*, *Opt. Acta*, **27** (1980) 321.
- [10] RICHY C. *et al.*, *J. Opt. Soc. Am. B*, **12** (1995) 456.
- [11] YARIV A. and YEH P., *Optical Waves in Crystals* (Wiley, New York, N.Y.) 1984, Chapt. 12.5.
- [12] BRUCKMEIER R. *et al.*, private communication (Universität Konstanz, Germany)
- [13] BOYD G. D. and KLEINMAN D. A., *J. Appl. Phys.*, **39** (1968) 3597.
- [14] PASCHOTTA R. *et al.*, *Opt. Lett.*, **19** (1994) 1325.
- [15] SCHILLER S. *et al.*, *Appl. Phys. Lett.*, **68** (1996) 3374.
- [16] COLLETT M. J. and WALLS D. F., *Phys. Rev. A*, **32** (1985) 2887; REYNAUD S. *et al.*, *Phys. Rev. A*, **40** (1989) 1440; FABRE C. and HOROWICZ R. J., *Opt. Commun.*, **107** (1994) 420.
- [17] CHABA A. N. *et al.*, *Phys. Rev. A*, **46** (1992) 1499.
- [18] PROTSSENKO I. E. and LUGIATO L. A., *Opt. Commun.*, **109** (1994) 304.
- [19] For travelling-wave cascaded quantum effects, see, *e.g.*, LI R. D. and KUMAR P., *Phys. Rev. A*, **49** (1994) 2157; BENCHEIKH K. *et al.*, *J. Opt. Soc. Am. B*, **12** (1995) 847; PERINOVÁ V. and LUKŠ A., *Acta Phys. Slov.*, **45** (1995) 395; BERZANSKIS A. *et al.*, *Opt. Commun.*, **118** (1995) 438.
- [20] BREITENBACH G. *et al.*, *J. Opt. Soc. Am. B*, **12** (1995) 2095.